A Resilient Kalman Filter Based Servo Clock

G. Giorgi and C. Narduzzi

Department of Information Engineering, University of Padova
via G. Gradenigo 6/b, Padova I-35131, Italy
e-mail: {giada.giorgi, claudio.narduzzi}@dei.unipd.it

***Abstract*—The accuracy level achievable with a given synchronization system is straightforwardly related to timestamp accuracy. Therefore, different methods have been proposed in the literature for reducing measurement uncertainty in synchronization systems. However, another important problem is deciding whether a received time information is trustworthy, particularly when timing messages generated by a supposedly reliable reference, point to significant discrepancies from the local clock. This paper presents a clock servo purposely designed for working with timestamps affected by sporadic outliers. The proposed algorithm is based on a Kalman filter (KF), whose correction phase has been modified so that the calculation of the a posteriori state vector estimate depends on the reliability of time offset and frequency deviation measurements, as assessed by an innovation-based outlier detector. To achieve greater robustness, two KF clock algorithms are run in parallel, a back-up servo providing usable state estimates whenever measurement information is withheld for too long times from the primary servo through being considered unreliable. The resulting composite algorithm features a much improved stability range, while retaining a very good accuracy.**

I. Introduction

Sharing a common time reference is an issue of primary relevance in distributed measurement systems. In the literature different solutions have been proposed for maintaining synchronization between network nodes. Some of these are well-suited for distributed systems based on a wired communication interface [1], [2] while others are purposely designed for wireless sensor networks [3], [4]. The former are usually based on a hierarchic synchronization network topology where a node, generally called master, distributes its time reference among its slave nodes. The latter are based instead on distributed synchronization protocols, where network nodes cooperate to achieve a common virtual time reference.

Any synchronization protocol is essentially based on a temporal succession of simple operations which basically consist in the exchange of timestamps between a pair of network nodes. From the knowledge of master timestamps each slave is able to estimate the time offset and the frequency deviation of its own local clock with respect to the master time reference. Frequency deviation in particular can be obtained from the knowledge of the time offset at the start and at the end of a time interval of known duration. These information are finally used for adjusting the local clock.

The accuracy level achievable with a given synchronization system is straightforwardly related to timestamp accuracy. However, another important problem is deciding whether a received time information is trustworthy, particularly when timing messages, generated by a supposedly reliable reference, point to significant discrepancies from the local clock. In fact, sudden large variations of the time offset can point either to unusual events affecting the local clock or to adverse conditions affecting the propagation of timing messages through the network. In the latter case messages should be flagged as unreliable but, in first place, such potential outliers have to be detected.

The problem of validating the contents of individual timing messages is seldom given explicit consideration (for instance, in [5]), as the effects of outliers are often assumed to be substantially filtered out within clock servo algorithms (e.g., [6]). Even so, however, such occasional large variations do affect the overall stability of the regulated local clock, resulting in performance degradation that prevents the achievement of good synchronization accuracy.

This paper presents a clock servo designed for working with timestamps affected by sporadic outliers. The proposed algorithm is based on a KF, whose correction phase has been modified so that the calculation of the *a posteriori* state vector estimate depends on the reliability of time offset and frequency deviation measurements, as assessed by the innovation-based detector. For this purpose, two KF clock algorithms are run in parallel. The main one normally discards measurements flagged as potential outliers, ensuring good stability of the regulated local clock as long as few outliers occur. The backup clock servo, instead, always accepts all measurement data, producing less accurate state estimates. Accordingly, it is not employed in normal conditions, but provides redundancy. Its purpose is to replace the *a posteriori* state estimate provided by the main clock whenever its innovation becomes so large as to endanger KF stability. The resulting composite algorithm features a much improved stability range, while retaining a very good accuracy.

II. Basic KF equations for clock servo

The Kalman filter is based on a set of equations that provide a recursive solution to a least-squares problem. The system model is represented in the form of the following equations:

Part of this work is supported by the Italian Ministry for Education, University and Research (MIUR) under PRIN Contract no. 2009ZTT5N4 001 ("Characterization and performance measurement in hybrid smart transducer networks: innovative experimental methods and instrumentation"

978-1-4799-0242-2/13/$31.00 ©2013 IEEE

TABLE I. KF-BASED CLOCK SERVO PARAMETERS

Parameter	Description
$\mathbf{x}(k) = [\theta(k), \gamma(k)]^T$	**State vector**. $\theta(k)$ and $\gamma(k)$ represent respectively the time offset and the frequency deviation in the two-state clock model.
$\mathbf{A} = \begin{bmatrix} 1 & \tau \\ 0 & 1 \end{bmatrix}$	**State matrix**. τ is the time step duration.
$\mathbf{u}(k) = 0$	**Input vector**. This is a null quantity since no input is provided to the clock state equations.
$\mathbf{B} = 0$	**Input matrix**. This is a zero matrix since $\mathbf{u}(k) \equiv 0$.
$\mathbf{z}(k) = [\hat{\theta}(k), \hat{\gamma}(k)]^T$	**Measurement vector**. $\hat{\theta}(k)$ and $\hat{\gamma}(k)$ are respectively the time offset and the frequency deviation measurements in correspondence to the k-th synchronization time instant.
$\mathbf{H} = \mathbf{I}$	**Measurement matrix**. This is the identity matrix.
$\mathbf{w}(k) = [\omega_\theta(k), \omega_\gamma(k)]^T$	**Process noise**. The first component is the random component associated to a white frequency noise, while the second corresponds to a random walk frequency noise in the clock model.
$Q = \begin{bmatrix} \sigma_\theta^2 & 0 \\ 0 & \sigma_\gamma^2 \end{bmatrix}$	**Process noise covariance matrix**. It is diagonal since processes $\omega_\theta(\cdot)$ and $\omega_\gamma(\cdot)$ are independent zero-mean processes with variances respectively equal to σ_θ^2 and σ_γ^2.
$\mathbf{v}(k) = [v_\theta(k), v_\gamma(k)]^T$	**Measurement noise**. The two random variables $v_\theta(k)$ and $v_\gamma(k)$ represent respectively the uncertainties associated to the two elements of the measurement vector $\mathbf{z}(k)$.
$R = \begin{bmatrix} u_\theta^2 & u_{\theta,\gamma} \\ u_{\theta,\gamma} & u_\gamma^2 \end{bmatrix}$	**Measurement noise covariance matrix**. It depends on the standard uncertainties u_θ and u_γ associated to the offset and frequency deviation measurements and on their covariance $u_{\theta,\gamma}$ which is non-zero, since both quantities are obtained from a common set of timestamps.

$$\mathbf{x}(k) = \mathbf{A}\mathbf{x}(k-1) + \mathbf{B}\mathbf{u}(k) + \mathbf{w}(k) \quad (1)$$
$$\mathbf{z}(k) = \mathbf{H}\mathbf{x}(k) + \mathbf{v}(k). \quad (2)$$

The first equation describes the evolution of the process, which depends on the vectors $\mathbf{x}(k)$ and $\mathbf{x}(k-1)$, representing respectively the local clock state at the k-th and $(k-1)$-th time instant, and on the input vector $\mathbf{u}(k)$. Matrices $\mathbf{A}$ and $\mathbf{B}$ are the state matrix and the input matrix. Finally, $\mathbf{w}(k)$ is the process noise vector.

The second equation is used to model the measurement process $\mathbf{z}(k)$. Here, $\mathbf{v}(k)$ is the measurement noise vector and the matrix $\mathbf{H}$ is the measurement matrix.

The Kalman filter operates in two phases. In the first, also called **prediction phase**, the *a priori* estimate of the state $\mathbf{x}(k)$ is obtained from the knowledge of the state at the previous time instant $k-1$ and the inputs $\mathbf{u}(k)$:

$$\hat{\mathbf{x}}^-(k) = \mathbf{A}\hat{\mathbf{x}}(k-1) + \mathbf{B}\mathbf{u}(k-1) \quad (3)$$
$$\mathbf{P}^-(k) = \mathbf{A}\mathbf{P}(k-1)\mathbf{A}^T + \mathbf{Q} \quad (4)$$

where $\hat{x}^-(k)$ is the *a priori* state estimate. $\mathbf{P}^-(k)$ is the *a priori* estimate error covariance matrix which can be determined by the *a posteriori* estimate error covariance $\mathbf{P}(k-1)$ and the process noise covariance matrix $\mathbf{Q}$.

The second phase consists in a **correction phase**, during which the *a posteriori* state estimate $\hat{\mathbf{x}}(k)$ and the *a posteriori* covariance matrix $\mathbf{P}(k)$ are obtained:

$$\mathbf{K}(k) = \mathbf{P}^-(k)\mathbf{H}^T \left(\mathbf{H}\mathbf{P}^-(k)\mathbf{H}^T + \mathbf{R}\right)^{-1} \quad (5)$$
$$\hat{\mathbf{x}}(k) = \hat{\mathbf{x}}^-(k) + \mathbf{K}(k)\left(\mathbf{z}(k) - \mathbf{H}\hat{\mathbf{x}}^-(k)\right) \quad (6)$$
$$\mathbf{P}(k) = \left(\mathbf{I} - \mathbf{K}(k)\mathbf{H}\right)\mathbf{P}^-(k) \quad (7)$$

$\mathbf{K}(k)$ is the Kalman gain, while $\mathbf{R}$ is the measurement noise covariance matrix. When the Kalman filter is used to implement a clock servo, filter parameters must be set as reported in Table I. A more detailed description of the basic KF-based servo clock can also be found in [7].

III. CLOCK MODEL AND MEASUREMENTS

The results reported in this paper are obtained mainly by simulation analysis, given the difficulty to reproduce in a repeatable experimental set-up the anomalies that might affect the time protocols and clock sources in a sensor network.

The behaviour of the unregulated local oscillator can be simulated by a model based on stochastic differential equations [8], [9]. In this paper a two-state discrete-time clock model is employed, by which the effect of clock stability on the performances of the synchronization protocol can be accurately analysed. Let $\theta(k)$ be the time offset and $\gamma(k)$ the fractional frequency deviation. Equations describing the evolution of clock state with a time step τ are:

$$\begin{cases} \theta(k) = \theta(k-1) + \tau \cdot \gamma(k) + \omega_\theta(k) \\ \gamma(k) = \gamma(k-1) + \omega_\gamma(k) \end{cases} \quad (8)$$

where $\omega_\theta(\cdot)$ and $\omega_\gamma(\cdot)$ are zero-mean processes with variances respectively σ_θ^2 and σ_γ^2. The corresponding clock time at the time instant $t_k = k \cdot \tau$ would be:

$$C(t_k) = \frac{1}{\nu_0} \cdot \left\lfloor \frac{t_k + \theta(k)}{1/\nu_0} \right\rfloor \quad (9)$$

where ν_0 is the nominal oscillator frequency. The Allan variance of the resulting free-running clock has been reported in Fig.1. Clock parameters have been set respectively as: $\sigma_\theta^2 = 10^{-18}$, $\sigma_\gamma^2 = 10^{-20}$ and $\nu_0 = 10$MHz, which are in good accordance with the actual clock parameters that can be found, for instance, in [10] or [11]. It is important to note that the main contribution at small time scales is due to the quantization effect and therefore it depends on the oscillator frequency: the greater the frequency and the lower the corresponding quantization noise. Larger time scales instead result to be affected by the presence of a random walk frequency noise.

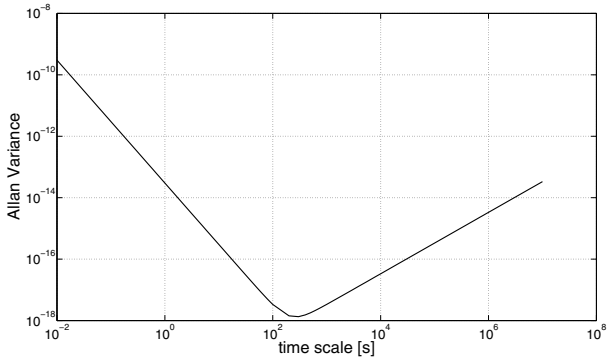

Fig. 1. Allan variance for the simulated clock model. The parameters of the clock are respectively: $\nu_0 = 10MHz$, $\sigma_\theta = 10^{-9}$, $\sigma_\gamma = 10^{-10}$.

To synchronized the local clock with respect to the reference time, both offset and frequency skew measurements are needed. As well known in literature, these values can be easily obtained through the timing messages exchanged by a pair of nodes [1], [2]. In particular the offset measurement $\hat{\theta}(k)$ provides the time offset between the two nodes in correspondence of the actual time instant t_k:

$$\hat{\theta}(k) = C(t_k) - t_k \tag{10}$$

while the frequency skew:

$$\hat{\gamma}(k) = \frac{\hat{\theta}(k) - \hat{\theta}(k-1)}{t_k - t_{k-1}} \tag{11}$$

is used to compensate for the difference between the actual frequency and the nominal frequency of the oscillator.

IV. Effect of outliers

In ideal situations timestamp inaccuracy results to be well-approximated by a white noise with finite variance. However, in a real context this hypothesis cannot be always satisfied and a better model is given by the sum of two or more random processes. A main process takes into account the uncertainty of timestamps under normal working conditions, while one or more contaminating processes are added to represent sporadically large deviations in the timestamping mechanism, that could variously be interpreted as inaccurate time measurements, delayed timestamps or some types of clock malfunctions.

Therefore, we model disturbances by adding a contaminating random process $n_B(k)$ in the KF measurement equations, so that timing information will occasionally be inaccurate. Measurement errors on the time offset estimate can thus be represented by the following model:

$$\hat{\theta}(k) = \theta(k) + v_\theta(k) + n_B(k), \tag{12}$$

where the additive term $n_B(k)$ is a random value with a given probability density function, generated with probability p.

A. Outliers: an example

Timing measurements affected by large errors give rise to a general loss of accuracy, as can be noted in the example of Fig. 2, where a basic Kalman filter is employed as the clock

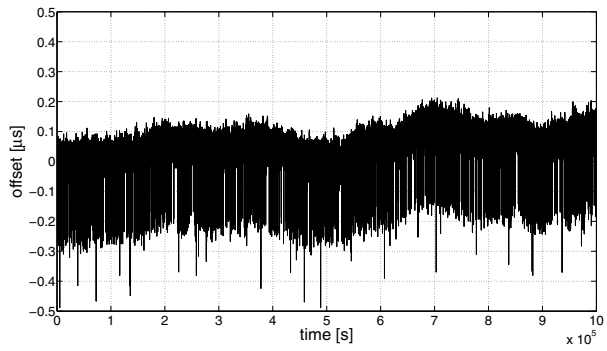

Fig. 2. Time offset of a local clock with a basic KF clock servo which receives timing messages at constant intervals. In this example, outliers have been modelled by a Bernoulli process with constant amplitude $n_B = 5\ \mu s$ and an occurrence probability equal to 0.1%. The free-running clock is the same of Fig. 1.

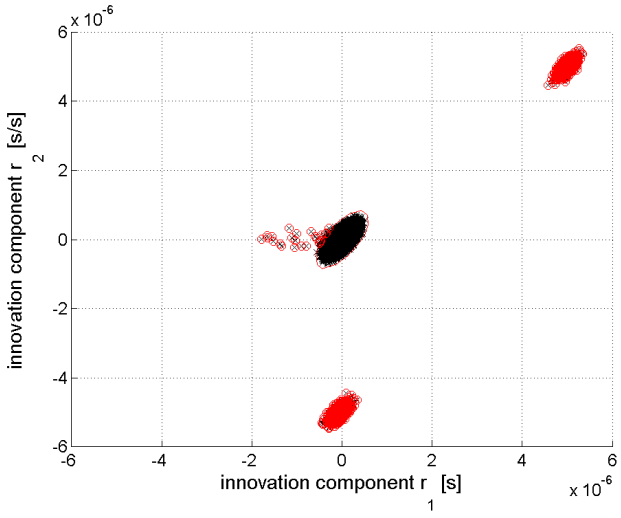

Fig. 3. Behaviour of the outlier detection algorithm [12]. The coverage probability associated to the acceptance region is equal to 95%.

servo. In this figure, the time offset between the local clock and the time reference is reported. The x-axis represents the reference time (also called master time), while in the y-axis the offset between the local clock and the time reference is reported. It is important to remark that this quantity is the actual offset of the regulated clocks, as it would be measured by an external observer. Simulation allows easy access to this quantity, that cannot be measured by the local clock itself. Therefore in practice it is impossible for the local clock to be aware of the presence of sporadic errors.

In these cases a basic KF clock servo is not sufficient for achieving better synchronization performances since it does not consider measurement reliability. On the other hand, even with accurate hardware timestamping the probability of measurement outliers can only be made lower, but not completely cancelled. Therefore, to increase robustness pre-processing of time measurements is needed.

V. RESILIENT KF-BASED SERVO CLOCK

In [12] a timestamp validation approach based on monitoring the innovation of a Kalman filter (KF) was presented. The KF is employed as a clock servo to calculate the corrected local time and a detector monitors the difference between the reference timestamp received through the network and the local KF-predicted time (i.e., the KF innovation process). The proposed detection criterion, based on a clear theoretical definition, was shown to be effective in discovering unusually large variations that may point to potentially unreliable data. This still leaves, as an open question, the decision whether information should be accepted regardless, or discarded accordingly. These alternatives illustrate the terms of a tradeoff, since accepting outliers may degrade the stability of the regulated clock, whereas discarding them may starve the KF of measurements, ultimately inducing instability and divergence of the regulated clock.

In the following subSection, the previously mentioned outlier detector is briefly described.

A. Outlier detection

Let $\mathbf{r}(k)$ be the difference between the actual measurement $\mathbf{z}(k)$ and its prediction $\mathbf{H}\hat{\mathbf{x}}(k)^-$:

$$\mathbf{r}(k) = \mathbf{z}(k) - \mathbf{H}\hat{\mathbf{x}}^-(k) \tag{13}$$

which is also called *innovation* or *measurement residual*.

When no anomalies affect the system, innovation is known to be a zero-mean white noise process, whose covariance matrix is:

$$\mathbf{S}(k) = \mathbf{H}\mathbf{P}^-(k)\mathbf{H}^T + \mathbf{R}. \tag{14}$$

Whenever new timing information are received, the corresponding measurement vector $\mathbf{z}(k)$ is obtained and the resulting innovation vector $\mathbf{r}(k)$ is computed, together with its covariance matrix $\mathbf{S}(k)$. From these, the squared Mahalanobis distance:

$$d_M^2(k) = \mathbf{r}^T(k)[\mathbf{S}(k)]^{-1}\mathbf{r}(k) \tag{15}$$

is computed. The acceptance criterion is:

$$d_M^2(k) \leq \eta_\alpha = -2\ln\alpha \tag{16}$$

the threshold η_α being associated to the desired level of confidence $(1-\alpha)$, determined from the asymptotic χ^2 distribution with two degrees of freedom that characterizes $d_M^2(k)$.

The detection condition is based on the dynamic system model (1) and highlights variations in the innovation process. If the inequality is not satisfied, measurement $\mathbf{z}(k)$ is flagged as a potential anomaly. The probability of a false alarm by the anomaly detector is equal to α. In practice, any variation in offset and/or fractional frequency deviation that appears so large as to be outside the physical possibilities of the local clock is regarded as suspect.

In Fig. 3 the behaviour of the outlier detector is described by a two-dimensional innovation plot. Residuals associated with measurements flagged as unreliable are drawn by circles. In this example the assumed level of confidence $1-\alpha$ is 95%, that corresponds to a threshold value $\eta_\alpha = 5.99$. The acceptance region resulting from (15) is delimited by an ellipse in the innovation plane, which is described by the quadratic form $\mathbf{r}^T(k)[\mathbf{S}(k)]^{-1}\mathbf{r}(k) = \eta_\alpha$.

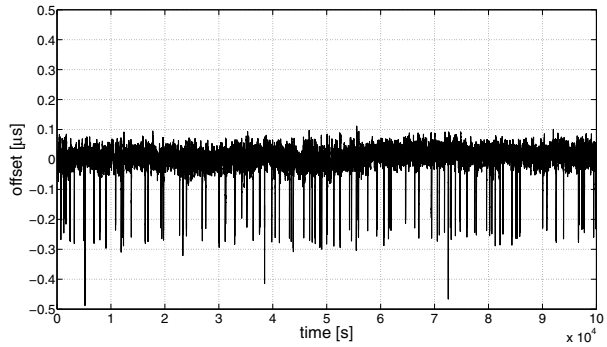

(a) Basic KF clock servo.

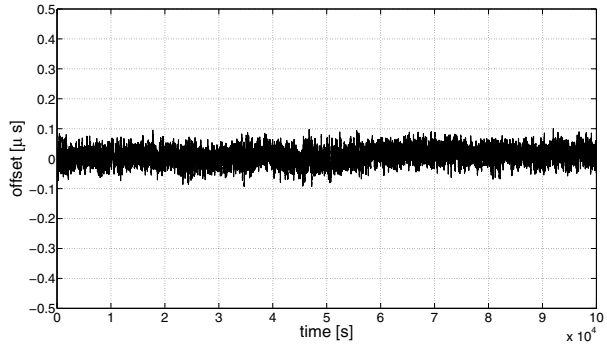

(b) KF clock servo with modified correction phase.

Fig. 4. Comparison between a basic KF clock servo and the modified clock servo (17). Outliers have been modelled by a Bernoulli process with constant amplitude $n_B = 5\ \mu s$ and an occurrence probability equal to 0.1%.

B. Outlier elimination

The outlier detector simply flags a measurement vector as a potential anomaly. This still leaves open the question about accepting or discarding such information. The latter alternative is possibly the simpler and corresponds to making use of measurement $\mathbf{z}(k)$ only if it is considered reliable. Otherwise, the *a priori* KF state prediction is taken as the updated clock state estimate:

$$\hat{\mathbf{x}}(k) = \begin{cases} \hat{\mathbf{x}}^-(k) & \text{if } d_M^2(k) \geq \eta_\alpha \\ \hat{\mathbf{x}}^-(k) + \mathbf{K}(k)\left(\mathbf{z}(k) - \mathbf{H}\hat{\mathbf{x}}^-(k)\right) & \text{otherwise} \end{cases} \tag{17}$$

A comparison between the behaviour of the KF-based servo with the basic and with the modified state estimate is shown in Fig. 4. The same timing measurements, received at a constant rate, have been employed with a basic KF clock servo (see Fig. 4(a)) and with a KF clock servo where the correction phase has been modified (see Fig. 4(b)) as described in (17). The comparison is referred to the time offset between the regulated local clock and the time reference, since this quantity is strictly related to synchronization accuracy.

It can be observed that, over the analysed time range between 0 and $100,000s$, the accuracy obtained by eliminating corrupted measurements is better. However, it must also be

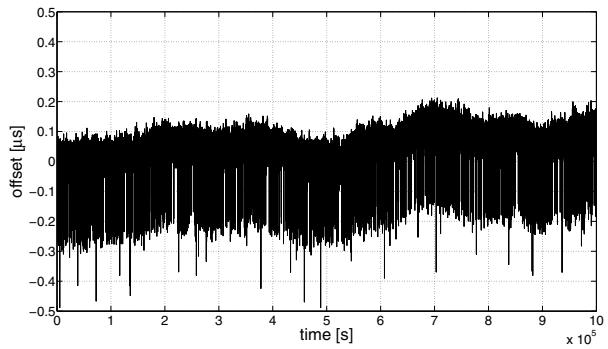

(a) Basic KF clock servo.

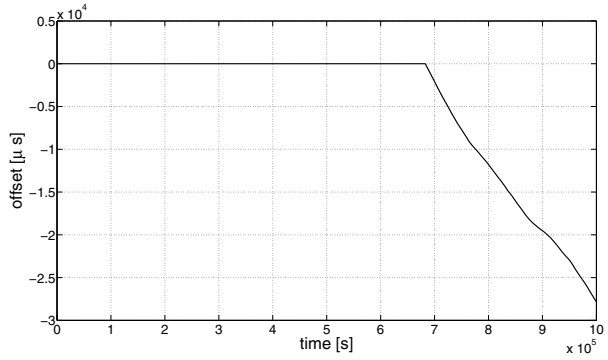

(b) KF clock servo with modified correction phase.

Fig. 5. Loss of clock by the modified KF clock servo (17). Reference time in the range between $0s$ and $10 \cdot 10^4 s$. Outliers have been modelled by a Bernoulli process with constant amplitude $n_B = 5\ \mu s$ and an occurrence probability equal to 0.1%.

noted that by discarding measurements in an unconscious manner, the modified KF may be starved of essential information and synchronization could eventually be lost. In fact, the ability to maintain synchronization depends on the stability of the local clock and on the accuracy of the KF filter state prediction $\hat{\mathbf{x}}^-(k)$ that replaces the update. These factors become increasingly critical when the number of detected outliers gets larger, or with long synchronization intervals, since the absence of measurements causes the KF state model to progressively "loose lock" on the actual evolution of the local clock. Fig. 5(b) refers to this case: as soon as the frequency deviation of the local clock begins to increase, measurements start to be discarded one after the other and synchronization is lost.

C. Improved outlier-aware clock servo

The proposed improved clock servo employs a composite algorithm, which maintains in parallel two regulated local clocks based on the same local oscillator. One of these regulated clocks provides the primary local time and generates local timestamps whenever required. The other is an auxiliary backup clock, that helps avoid total loss of synchronization. Both clocks employ a KF-based clock servo, with different state update equations. Specifically, the backup clock employs the unmodified equation (5), which allows to preserve some synchronization with the time reference, although with limited accuracy if outliers become larger and more frequent.

Each time a new measurement is provided by the synchronization protocol, a check is done. Measurements that are flagged as unreliable are not used for updating the Kalman filter, as previously described. normally, unreliable measurements are replaced by the a priori state estimate, as in (17). However, if the number of discarded measurements exceeds a given guard value, the state variable $\hat{\mathbf{x}}$ is forced instead to assume the same value of the *a priori* state estimate of the backup clock.

The primary clock refers therefore to the following modified KF update equations:

$$\hat{\mathbf{x}}(k) = \begin{cases} \hat{\mathbf{x}}^-(k) \ \text{ if } \ \left(d_M^2(k) \geq \eta_\alpha\right) \wedge \left(c(k) < \Delta\right) \\ \hat{\mathbf{x}}^-_{backup}(k) \ \text{ if } \ \left(d_M^2(k) \geq \eta_\alpha\right) \wedge \left(c(k) \geq \Delta\right) \\ \hat{\mathbf{x}}^-(k) + \mathbf{K}(k)\left(\mathbf{z}(k) - \mathbf{H}\hat{\mathbf{x}}^-(k)\right) \ \text{ otherwise} \end{cases} \tag{18}$$

where $c(\cdot)$ is a counter used for keeping track of the number of discarded measurements. In particular, $c(k)$ provides the number of consecutive discarded measurement at the k-th time instant. Δ is the guard value which is a parameter of the proposed algorithm. Its value must be carefully set since it affects the capability of the proposed clock servo to keep the local clock synchronized to the master time also in presence of a given number of consecutively discarded measurements.

The time behaviour of the offset from the the time reference achieved by the local clock with the improved outlier-aware clock servo is illustrated in Fig. 6. The results reported in this figure have been obtained by executing the proposed clock servo in parallel with the other two clock servos, whose performances have been illustrated respectively in Figs. 4(a) and 4(b), so that exactly the same sequence of timing messages was involved.

As can be noted, when the first $60 \cdot 10^4 s$ from the starting time instant $(t = 0)$ are considered in Fig. 6(a) it is immediate to see that the time offset is approximately the same as in Fig. 4(b). In fact in this interval the number of outliers that are discarded is small enough to prevent synchronization loss by the local clock. However, the different behaviour of the two clock servos is clearly evidenced when synchronization starts to be lost about $68 \cdot 10^4 s$ from the initial time instant, as shown in Fig. 5(b).

In the first case, where no control is introduced on the maximum number of discarded timing measurements, synchronization is lost and the time offset between the local clock and the time reference diverges. In the second case instead when the number of discarded timing measurements becomes greater than the guard value $\Delta = 10$, synchronization is forced by using the information provided by the backup clock. This results anyway in a worsened synchronization accuracy, as can be noted by analysing the results given in Fig. 6(a): under normal working conditions the time offset is between $-200\ ns$ and $+200\ ns$, while when the backup clock is used the time offset increases and assumes values in the range within $-2\ \mu s$ and $+500\ ns$. For this reason, when the backup clock is used, an alarm is also generated, as reported in Fig. 6(c). This warning signal can be used by applications that make use of the synchronized local clock to take into account the accuracy

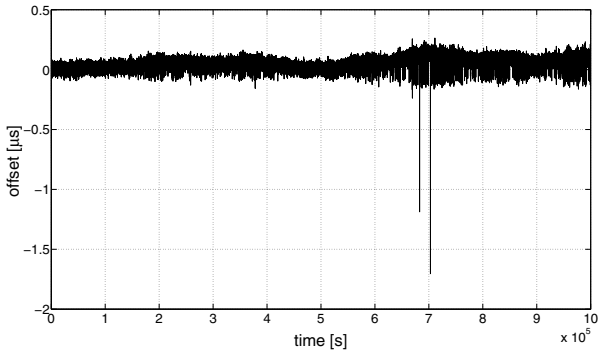

(a) Time offset between local clock and time reference.

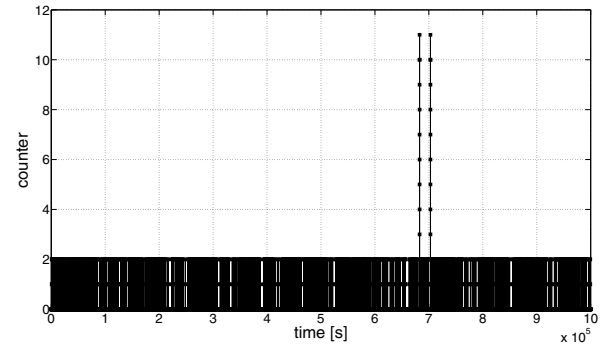

(b) Counter.

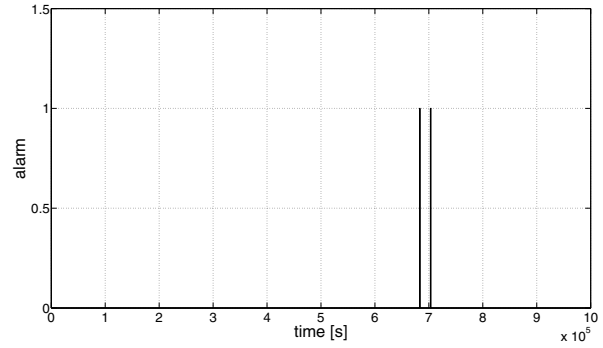

(c) Alarm.

Fig. 6. This analysis refers to a clock, which receives timing messages at constant intervals. the contaminating process has been modelled by a Bernoulli noise process with constant amplitude $n_B = 5$ μs.

degradation due to the presence of a large number of corrupted timing measurements.

VI. Conclusion

Validation of individual timing messages in a network synchronization protocol is a long-standing problem. Different approaches have been proposed to deal with the issue, where heuristics based on experience and general engineering criteria have been applied.

In the proposed KF-based approach, resilience to measurement outliers has been achieved by coupling a rigorously justified statistical test on incoming measurement information with a redundant clock servo algorithm. This gives the implemented regulated clock the capability to preserve its lock to the reference time with much enhanced robustness. It allows as well to signal temporary accuracy degradation to any dependent application.

Future development of this work will focus on enhancing the integration between the primary and back-up servos, to further improve the stability and accuracy of the regulated local clock.

References

[1] D. L. Mills, *Network Time Protocol (Version 3) Specification, Implementation and Analysis*, IETF Network Working Group, RFC 1305, March 1992.

[2] International Standard IEEE1588, *Precision clock synchronization protocol for networked measurement and control systems*, IEEE Std. 1588:2008.

[3] R. Carli, S. Zampieri, *Networked clock synchronization based on second order linear consensus algorithms*, *Proc. of the IEEE Conference on Decision and Control*, pp. 7259 - 7264 , December 2010.

[4] Y.C. Wu, Q. Chaudhari, E. Serpedin, *Clock Synchronization of Wireless Sensor Networks*, IEEE Signal Processing Magazine, January 2011, pp.124-138.

[5] D. Veitch, S. Babu, A. Pástor, *Robust synchronization of software Clocks Across the Internet*, Proc. of the 4th ACM SIGCOMM Conf. on Internet Measurement, pp. 219-232, 25-27 Oct. 2004, Taormina, Sicily, Italy.

[6] N. Barendt, K. Correll, M. Branicky, *Servo Design Considerations for Software-only Implementations of the Precision Time Protocol*, Proc. Workshop on IEEE 1588, 10-12 October 2005.

[7] G. Giorgi, C. Narduzzi, "Performance analysis of Kalman filter-based clock synchronization in IEEE 1588 networks", *IEEE Trans. on Instrumentation and Measurement*, vol. 60, n. 8, pp. 2902-2909, Aug. 2011.

[8] L. Galleani, L. Sacerdote, P. Tavella, C. Zucca, *A mathematical model for the atomic clock error*, Metrologia, vol. 40, no. 3, pp. S257-S264, Jun. 2003.

[9] W. J. Riley, *Handbook of Frequency Stability Analysis*, NIST, Special Publication 1065, July 2008.

[10] F. Ring, G. Gaderer, A. Nagy,P. Loschmidt, "Distributed Clock Synchronization in discrete Event Simulators for Wireless Factory Automation", *Proc. International IEEE Symposium on of Precision Clock Synchronization for Measurement Control and Communication (ISPCS 2010)*, pp. 103-108, IEEE, 2010.

[11] H. Abubakari, S. Sastry. "IEEE 1588 style synchronization over wireless link". *Proc. IEEE International Symposium on Precision Clock Synchronization for Measurement, Control and Communication, 2008. (ISPCS 2008)*, pp. 127-130, IEEE, 2008.

[12] M. Bertocco, G. Giorgi, C. Narduzzi, *Innovation-based Timestamp Validation for Reliable Sensor Network Synchronization*, Proc. of the IEEE International Instrumentation and Measurement Technology Conference, I2MTC 2013, Minneapolis MN, 6-9 May 2013.